Development of a vernix caseosa substitute : a novel strategy to improve skin barrier function and repair

Rißmann, R.

2

New insights into ultrastructure, lipid composition and organization of vernix caseosa

Robert Rissmann[1], Wouter Groenink[1], Arij Weerheim[2], Steven Hoath[3], Maria Ponec[1] and Joke Bouwstra[1]

[1] Department of Drug Delivery Technology, Leiden/ Amsterdam Center for Drug Research
[2] Department of Dermatology, Leiden University Medical Center
[3] Skin Sciences Institute, Children's Hospital Research Foundation, University of Cincinnati, USA

Adapted from *Journal of Investigative Dermatology* 2006; 126: 1823-1833

Abstract

The upper layer of the epidermis, the stratum corneum, is very important for skin barrier function. During the last trimester of gestation, the stratum corneum of the fetus is protected by a cheesy, white biofilm called vernix caseosa. It consists of water containing corneocytes embedded in a lipid matrix and the basic structure shows certain similarities to stratum corneum. The present study aimed to characterize vernix caseosa, with main focus on an integral analysis of free and (to the corneocytes) bound lipids, on the lipid organization, and on ultrastructure. Free lipids of vernix caseosa show a wide distribution in polarity; nonpolar lipids such as sterol esters and triglycerides predominate having a chain length up to 32 carbon atoms. The profile of fatty acids, ω-hydroxyacids and ω-hydroxyceramides – representing the bound lipids of vernix caseosa – shows high similarity with that of stratum corneum. Morphological studies revealed the presence of highly hydrated corneocytes embedded in lipids, the latter being occasionally accumulated as lipid pools. Freeze fracture electron microscopy showed smooth surfaces of corneocytes and a heterogeneous appearance of intercellular lipids. The results suggest a lower degree of ordering of vernix caseosa lipids as compared to the stratum corneum. A small-angle X-ray diffraction study showed similar results.

Introduction

Vernix caseosa (VC) is a white, greasy biofilm, which covers large skin areas of the fetus during the last trimester of pregnancy and is often still present on the skin during delivery. The beginning of VC formation coincides with the onset of epidermal differentiation and barrier formation *in utero*, around gestation week 24 [1]. *In utero,* VC forms a unique barrier between the amniotic fluid and the fetus, where the required functions are very different from the postnatal environment [2]. VC consists of hydrophilic corneocytes embedded in a lipid matrix and thus its basic structure shows similarities to that of SC. Morphological studies of VC showed that it is comprised of ovoid or polygonal, malleable corneocytes surrounded by lipids [3]. These intercellular lipids contain unidentified inclusion bodies with uncertain origin. The cellular part of VC is suggested to be derived from detached SC corneocytes, and the intercellular connections, the desmosomes, are lacking [4]. Furthermore, Pickens *et al.* [4] showed that most of the water is situated within the corneocytes and proposed a second water compartment in granular inclusions within the lipids. Besides 80% of water, VC is composed of about 10% proteins and 10% lipids in its natural environment [4, 5].

Lipids are key factors for the barrier properties of the SC. Extractable, free lipids are present in the intercellular space and bound lipids are covalently linked to the

cornified envelope. In SC the free lipids mainly consist of cholesterol (CHOL), ceramides (CER) and free fatty acids (FFA), forming two co-existing lamellar phases with a repeat distance of 6 and 13 nm, respectively [6]. In VC the lipid composition is different. Haahti *et al.* [7] and Kaerkkaeinnen *et al.* [8] provided the first information on the free lipid composition in VC. Major fractions could be identified containing sterol esters (SE) and triglycerides (TG). In addition, Kaerkkaeinnen *et al.* [8] showed that the fatty acids of individual lipid classes, such as SE, wax esters (WE) and TG, consist of straight and methyl branched fatty acids. Subsequent studies confirmed these results [9] and provided information on the double bond positions and more detailed information on the fatty acid composition [10, 11]. However, very long chain fatty acids were often neglected as most of these studies were carried out focusing on acyl chain length distribution up to a length of 20 carbon atoms. In addition to the common SC CER, Oku *et al.* [12] identified the presence of two additional CER. Furthermore, Hoeger *et al.* [5] found that all barrier lipids of SC are present in VC. All studies performed until now were fragmented, focusing either on the nonpolar free lipids SE, WE and TG or on the barrier lipids of VC, in particular on the CER. Currently, no data on the overall free lipid composition of VC are available in literature. Moreover, no information on the composition of bound lipids in VC is available. Very interestingly, recently it was observed that the FFA in VC exhibit antibacterial activity [13].

The objective of our study was to characterize VC in more detail, with a main focus on the overall analysis of all lipid classes present in VC and the profile of the fatty acids up to a chain length of 32 carbon atoms using high performance thin layer and gas chromatography. Besides the free lipid composition, a detailed analysis of the bound lipids was also carried out. Ultrastructural studies using cryoscanning electron microscopy were aimed to gather more knowledge on the water distribution within the VC. Lipid organization was investigated by freeze fracture electron microscopy (FFEM) and small-angle X-ray diffraction (SAXD).

Materials & Methods

Collection and preparation of vernix caseosa and stratum corneum

VC was scraped off gently immediately after vaginal delivery or caesarean section of healthy term neonates. The samples were directly transferred into sterile plastic tubes, and stored at 4ºC until use. The collection of VC was conducted after informed consent of the mother and was approved by the ethical committee of the University Hospital Cincinnati and the Leiden University Medical Center.

Abdomen or breast skin was obtained after cosmetic surgery from local hospitals with the informed consent of the patients. Subcutaneous fat tissue was removed, after which the skin was carefully cleaned with tissue paper, which was prior soaked in 70% ethanol. Then the skin was dermatomed to a thickness of approximately 300 µm (Padgett Electro Dermatome Model B, Kansas City, USA). SC was isolated by incubating the dermal side of the skin on trypsin soaked filter paper as described elsewhere [14]. The SC was subsequently washed several times with water and then stored in a silica gel containing desiccator under nitrogen. All samples were taken with adherence to the Helsinki Guidelines.

Lipid extraction and analysis

VC samples from 9 healthy neonates were used for extraction. Free lipids of VC were extracted by a modified method of Bligh & Dyer [15]. In short, the samples were extracted with chloroform/methanol mixtures (2:1, 1:1, 1:2, v/v), respectively. This procedure was repeated until complete extraction of free lipids was achieved. The fractions were combined and the lipid extract was stored at -20˚C until use. Bound lipids of VC were collected after mild saponification of the residue (remaining after extraction of free lipids) with 1M NaOH in 90% methanol at 60˚C for 2 h [16], and subsequently extracted, as mentioned above. Analysis of lipid composition was performed by one-dimensional, horizontal HPTLC as described before [5, 17]. Serial dilutions of appropriate standards were used for quantification. The standards comprised of squalene (SQ), cholesteryl oleate representing SE, oleyl oleate representing WE, glycerol trioleate representing TG, CHOL, palmitoleic acid representing FFA, cholesterol sulphate (CSO_4) and synthetic CER, consisting of an acyl-CER (CER(EOS)), two nonhydroxy-CER (CER(NS) and CER(NP)) and an α-hydroxy-CER (CER(AP)) according to the terminology of Motta *et al.* [18].

The CER were kindly provided by Cosmoferm B.V. (Delft, The Netherlands). All other compounds were purchased from Sigma Aldrich GmbH (Schnelldorf, Germany). All used organic solvents were of analytical grade and manufactured by Labscan (Dublin, Ireland).

The quantification was performed after staining (copper acetate and copper sulphate in phosphoric acid) and charring at 170°C using a digitalized photo (BIO-RAD scanner GS710) and the software QuantityOne®. Three parallel samples were used for quantification; all data are presented as means ± SD (w/w) %.

Preparation and analysis of fatty acid methyl esters

Fatty acid methyl esters (FAME) of VC were analyzed according to the method as reported earlier [19, 20]. Briefly, in order to determine fatty acid composition of individual lipid fractions, extracts of free and bound lipids were separated by HPTLC and several fractions were scraped off, extracted and transmethylated in 1 ml of 10% boron trichloride in methanol using microwave irradiation. FAME were dissolved in hexane and purified on silica-gel column, as described earlier [17]. This system allowed separation of the FAME and alcohols together with hydroxyl-FAME. FAME fractions containing either nonhydroxy (methyl branched or straight) fatty acids, α-hydroxyacids or ω-hydroxyacids were analyzed with a Vega GC 6000 gas chromatograph (Carlo Erba Instruments, Milan, Italy) using a CP Wax 52 capillary column (Chrompack, Varian, Bergen Op Zoom, the Netherlands). An initial temperature of 80°C was increased to 160°C at a rate of 10°C per min followed by a 2°C per min increase to 250°C, which was maintained until all components were eluted. The peaks were identified using the following standards: fatty alcohols, straight non-hydroxy fatty acids, ω-1 methyl branched (iso) fatty acids, ω-2 methyl branched (anteiso) fatty acids, α-hydroxyacids (all Alltech; Breda, The Netherlands), synthetic ω–hydroxyacids (Cosmoferm B.V., Delft, The Netherlands) and natural ω–hydroxyacids from carnauba wax [16]. Integration of peak areas and calculation of weight percentages was performed by a Baseline 810 integrator. Heptadecanoic acid was used as the internal standard. To correct for background, lipid-free samples underwent the same separation and transmethylation procedure (HPTLC development, off-scraping, extraction from silica gel and final column separation) and appropriate peak areas were subtracted in analyzed lipid samples. To refine the identification of individual components, samples and standards were also injected simultaneously to confirm the data obtained with the external standards. Alcohols and ω-hydroxyacids of the hydroxy FAME were converted by acetylation with acetanhydride to their analogical ester. Due to acetylation a shift in the retention time occurred. This allowed confirmation of results obtained with external standards.

Cryoscanning electron microscopy

A small amount of VC (~2 mg) was placed in a small cylindrical sample holder and further processed, as described in detail elsewhere [21]. Briefly, the samples were rapidly frozen at -180°C in liquid propane using the plunging method (KF80, Reichert-Jung, Vienna, Austria). The cryo-fixed samples were sliced at a specimen temperature of –90°C and the samples were freeze dried for 1 min at -90°C at 0.1 Pa and sputter coated with 5 nm Platinum. The samples were

mounted into a field emission electron microscope (6300 FESEM, Yeol, Tokyo, Japan) and examined at -190°C.

Freeze fracture electron microscopy
VC samples were fixed between two copper plates and immediately cryo-fixed in liquid propane. The frozen specimens were stored in liquid nitrogen until further use. The fracture of the samples was performed by a slightly modified method as described elsewhere [22]. Briefly, the samples were mounted onto a special designed sample holder and then placed on a precooled table (-150°C) in a Balzers BAF 400-D freeze fracture device (Balzers, Lichtenstein). The samples were fractured and replicated by evaporation of platinum and carbon. The replicas were removed from the freeze fracture device and subsequently cleaned by submersion into 0.5 M quaternary ammonium hydroxide in toluene (Soluene™-350, Packard, Groningen, The Netherlands) followed by washing with toluene. The replicas were visualized in a Philips EM410 (Philips, Eindhoven, The Netherlands) transmission electron microscopy system.

Small-angle X-Ray Diffraction
SAXD measurements were conducted at station BM26B at the European Synchrotron Radiation Facility in Grenoble, France [23] and the measurements were carried out as described earlier [24]. The diffraction data were collected by a two-dimensional gas-filled area detector. The diffraction pattern was obtained at room temperature for a collection period of 5 min. Duplicate measurements of VC samples were performed to confirm reproducibility.

Results
Nonpolar lipids dominate in VC
The free lipid fraction was extracted from VC and separated by HPTLC. The extracted free lipid fraction comprised of 11.1 ± 2.4% of total weight of VC. Free lipids extracted from VC were separated by means of HPTLC. As shown in figures 1A and 1B, VC consists of a wide spectrum of lipid classes. Barrier lipids, i.e. CHOL, FFA and CER, represent approximately 10% of total lipids, whereas in SC they represent the major lipid classes (about 80%). Nonpolar lipids including SE, WE, DIOL and TG are the dominant components of the VC. The most abundant are SE/WE (42.0 ± 7.5%) and TG (35.9 ± 5.5%). In SC the CER (36.0 ± 3.2%) are the predominant fraction followed by FFA (23.6 ± 4.7%) and CHOL (18.9 ± 5.3%). Although SC from *ex vivo* skin was thoroughly ethanol wiped, sebum components such as TG and SE/WE were also found to be present in small amounts.

VC consists of the same CER classes as SC

The total CER content of VC was 4.9 ± 1.6% of total free lipids. Chromatographic separation showed the presence of 8 CER classes in VC and SC (Fig. 1A and 1C). The development system did not allow the separation of CER(AS) and CER(NH). In agreement with Hoeger *et al.* [5] CER(AH) is with 22.0 ± 6.6% the most prominent CER in VC. Slightly lower levels of CER(NS) (19.5 ± 5.9%), CER(AS/NH) (17.3 ± 3.3%) and CER(EOS) (14.8 ± 6.0%) were observed. The CER(EOP) content was low but still detectable (2.7 ± 1.1%). The CER profile in SC was similar with exception of CER(NP), being present in higher amounts (21.5 ± 0.9%).

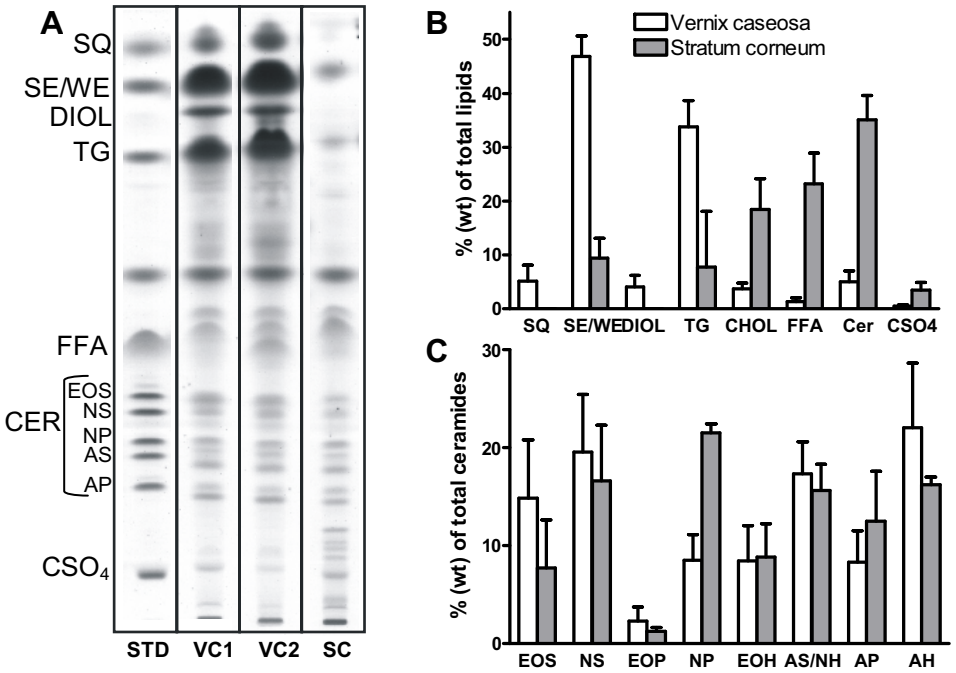

Figure 1. Next to barrier lipids, vernix caseosa (VC) contains a high amount of nonpolar lipids. Developed and charred HPTLC plate shows a standard solution, two VC samples and free lipid extracts of stratum corneum (SC) (panel A). Photo densitometry allowed quantitative analysis of the free lipid extracts for all VC compounds (panel B) and the ceramides separately (panel C). Results are shown as weight percentage +SD (n=7).

Fatty acids of VC consist of both branched and straight chains with a chain length variation between 14 and 32 carbon atoms

HPTLC separation of VC lipid extracts allowed isolation of six different fatty acid containing fractions (SE, combined fraction of SE and WE (SE/WE), WE, DIOL, TG and FFA) (Fig. 2). In each of these fractions gas chromatography analysis of FAME revealed a wide distribution of fatty acids with carbon chain length varying between C14 and C32. The fatty acids consist of straight saturated and unsaturated (cis and trans) fatty acids, iso and anteiso branched fatty acids and α- and ω-hydroxyacids. The identified fatty acids of the individual fractions are shown in table 1 and 2. A high number of various standards were used to identify the GC peaks (alcohols, straight, iso and anteiso, cis and trans monounsaturated fatty acids and α- and ω-hydroxyacids and alcohols). This resulted in identification of the majority of components. However, even with a high number of standards used for identification, about 22.3% of total fatty acids still remained unknown. This fraction comprised 8.3% of fatty acid with chain length shorter than C20, 8.3% with a chain length of C20-C30 and 5.7% with a chain length above C30. The fraction of SE contains the highest amount of branched fatty acid (55.6%) and only a small amount of α- and ω-hydroxyacids. The fraction of WE comprises more straight fatty acids including the highest content of unsaturated fatty acids (29.0 ± 8.2%). DIOL is characterized by an almost balanced relative content of saturated (20.0 ± 5.1%), unsaturated (16.6 ± 9.5%), iso (13.8 ± 2.1%) and anteiso (13.5 ± 0.3%) fatty acids. The fractions of TG and FFA are featuring a much higher prevalence of straight chains (43.1% and 60.3%, respectively) over branched chains (19.8% and 20.8%, respectively).

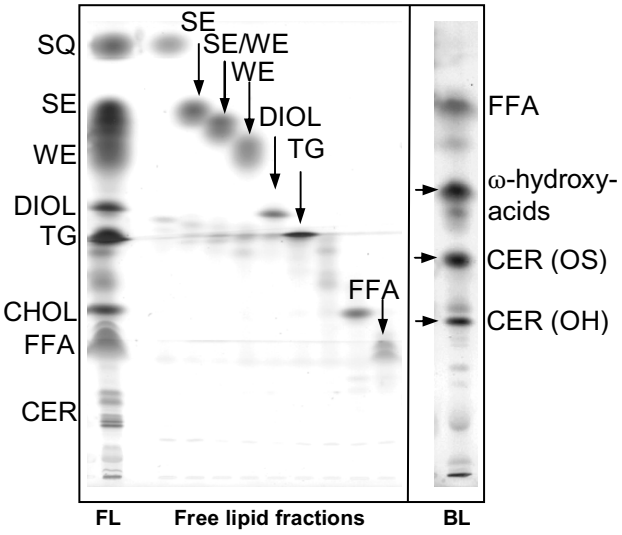

Figure 2. Chromatographic separation of VC lipids. HPTLC plates show the free lipid extract (FL, left), its fractions and bound lipids (BL, right) which were subjected to GC analysis (arrows).

Table 1. Fatty acid distribution in vernix caseosa lipid fractions (weight% ±SD per fraction, n=6)

compound	SE	SE/WE	WE	DIOL	TG	FFA
straight saturated	7.1 ±1.6	16.7 ±6.0	14.8 ±1.8	20.0 ±5.1	18.3 ±9.3	40.5 ±15.8
straight unsaturated	14.0 ±2.0	16.3 ±1.8	29.0 ±8.2	16.6 ±9.5	24.8 ±6.0	19.8 ±8.0
branched iso	29.0 ±2.5	12.9 ±0.3	7.7 ±0.4	13.8 ±2.1	9.8 ±5.0	12.2 ±0.4
branched anteiso	26.6 ±1.9	10.3 ±3.3	8.5 ±9.1	13.5 ±0.3	10.0 ±0.2	8.6 ±0.7
α-hydroxyacids	0.9 ±0.3	10.7 ±7.4	8.5 ±6.9	6.6 ±2.9	2.5 ±0.7	-
ω-hydroxyacids	1.6 ±0.7	3.9 ±0.4	2.3 ±0.9	4.4 ±4.1	6.3 ±0.6	2.6 ±0.5
alcohols	2.7 ±2.6	10.8 ±7.0	16.8 ±15.9	8.6 ±4.1	6.2 ±3.4	-

SE– sterol ester, WE–wax ester, DIOL–dihydroxy wax esters, TG–triglycerides, FFA–free fatty acids, c-cis, t- trans

Table 2. Chain length distribution in various free lipid fractions (weight% ±SD per fraction, n=6)
A. Straight chain fatty acids

chain length	SE	SE/WE	WE	DIOL	TG	FFA
saturated						
14	-	0.4 ±0.5	0.1 ±0.2	0.9 ±1.2	0.9 ±0.8	-
15	0.2 ±0.2	0.8 ±0.6	0.1 ±0.1	1.2 ±1.7	0.3 ±0.3	6.2 ±2.7
16	0.8 ±0.8	1.2 ±1.7	3.6 ±4.0	6.5 ±9.1	10.8 ±7.4	24.6 ±12.7
18	1.1 ±0.1	0.4 ±0.6	0.6 ±0.8	1.8 ±0.5	2.0 ±0.6	4.2 ±0.9
19	0.4 ±0.0	-	4.4 ±6.2	3.7 ±4.1	0.5 ±0.1	0.9 ±0.2
20	0.4 ±0.6	0.3 ±0.3	0.7 ±0.2	1.0 ±0.6	0.5 ±0.0	0.7 ±0.1
21	-	0.1 ±0.1	0.1 ±0.1	0.4 ±0.2	0.4 ±0.0	0.3 ±0.0
22	-		3.4 ±1.9	-	-	-
23	-	0.2 ±0.3	-	2.0 ±0.9	0.2 ±0.2	1.3 ±0.1
24	0.8 ±1.1	0.3 ±0.5	0.1 ±0.2	1.0 ±0.1	0.4 ±0.0	-
25	2.8 ±2.8	4.6 ±2.1	1.1 ±1.5	1.3 ±0.7	0.4 ±0.1	1.7 ±0.0
26	0.1 ±0.1	0.3 ±0.5	0.2 ±0.3	0.1 ±0.1	0.1 ±0.0	-
27	0.6 ±0.7	0.9 ±1.2	0.4 ±0.3	-	1.3 ±0.1	0.6 ±0.1
32	-	7.3 ±10.3	-	-	-	-
unsaturated						
16:1t	0.2 ±0.3	0.3 ±0.4	0.6 ±0.8	2.6 ±3.6	10.9 ±4.8	8.5 ±1.6
16:1c	0.3 ±0.0	0.5 ±0.5	16.5 ±0.6	3.6 ±1.1	3.1 ±3.2	0.6 ±0.8
18:1t	0.4 ±0.4	6.2 ±2.5	0.3 ±0.4	3.7 ±3.7	4.4 ±4.5	5.7 ±3.2
18:1c	0.8 ±0.0	1.8 ±0.5	3.2 ±0.7	4.3 ±3.9	4.2 ±2.8	2.7 ±1.1
18:2t	0.5 ±0.6	0.1 ±0.2	0.2 ±0.3	-	0.8 ±0.0	-
18:2c	-	0.1 ±0.1	6.3 ±7.0	1.0 ±0.9	0.3 ±0.3	1.1 ±0.8
20:1c	1.9 ±0.3	2.1 ±0.6	0.9 ±0.8	0.7 ±0.5	0.2 ±0.0	0.3 ±0.1
22:1t	2.6 ±3.7	2.6 ±0.5	0.2 ±0.3	-	0.3 ±0.1	0.3 ±0.2
22:1c	5.1 ±1.6	0.6 ±0.8	0.2 ±0.3	0.7 ±0.5	0.4 ±0.0	-
24:1t	-	0.5 ±0.7	0.4 ±0.6	-	-	-
24:1c	2.1 ±3.0	1.4 ±0.1	-	-	0.3 ±0.4	0.6 ±0.2

Table 2 (continued). Chain length distribution in various free lipid fractions of vernix caseosa (weight% ±SD per fraction, n=6)
B. Branched chain fatty acids

chain length	SE	SE/WE	WE	DIOL	TG	FFA
iso						
14	0.4 ±0.6	0.5 ±0.8	0.3 ±0.4	1.0 ±0.6	0.1 ±0.1	
16	3.0 ±0.0	3.9 ±3.3	3.2 ±1.7	2.8 ±4.0	3.7 ±3.4	3.2 ±1.9
18	1.0 ±1.5	0.6 ±0.1	1.5 ±0.3	1.5 ±1.0	1.8 ±0.2	2.0 ±1.7
20	13.0 ±0.8	0.8 ±1.0	-	4.0 ±0.4	0.3 ±0.0	0.3 ±0.2
22	-	-	-	0.3 ±0.0		
23	2.9 ±4.0	-	-	-		
24	0.8 ±0.7	0.3 ±0.2	2.6 ±1.6	1.3 ±0.8	0.5 ±0.3	5.6 ±0.4
25	2.7 ±3.8	1.3 ±0.2		1.2 ±0.2	0.5 ±0.6 -	
26	2.4 ±3.1	1.5 ±2.0	-	-	-	
27	0.5 ±0.8	1.1 ±0.9	-		0.2 ±0.2	1.0 ±0.3
28	1.9 ±2.6	1.2 ±1.7	0.1 ±0.1	-	-	
29	0.3 ±0.5	1.4 ±2.1	-	0.1 ±0.2		0.2 ±0.1
30	-	0.1 ±0.2	0.1 ±0.0	1.7 ±0.8	2.5 ±0.2	-
anteiso						
15	0.2 ±0.3	1.9 ±2.3	0.7 ±0.5	1.4 ±1.5	0.1 ±0.1	1.4 ±0.1
16	-	0.3 ±0.4	1.2 ±1.6	-	1.7 ±0.2	0.7 ±0.4
17	0.8 ±1.1	1.4 ±0.7	1.3 ±1.5	0.7 ±1.0	0.2 ±0.2	1.2 ±0.2
18	1.0 ±1.5	-	3.7 ±4.9	1.0 ±1.0	0.5 ±0.0	0.7 ±0.1
21	7.5 ±0.5	0.9 ±0.8	-	0.6 ±0.3	0.2 ±0.1	0.4 ±0.1
22	12.4 ±0.2	1.3 ±1.8	0.1 ±0.1	4.6 ±0.3	0.5 ±0.2 -	
23	-	1.3 ±0.4	-	0.3 ±0.4		0.8 ±0.2
24	3.4 ±4.8	1.1 ±1.1	0.5 ±0.7	0.3 ±0.2	-	
26	0.6 ±0.1	0.4 ±0.6	0.9 ±1.2	4.7 ±2.0	4.8 ±0.3	3.3 ±0.2
27	0.8 ±0.7	1.6 ±2.4	0.1 ±0.2	-	1.8 ±0.1	

SE– sterol ester, WE–wax ester, DIOL–dihydroxy wax ester, TG–triglycerides, FFA–free fatty acids, c-cis, t- trans

Bound lipids of VC consist of CER(OS), CER(OH), fatty acids and ω-hydroxyacids

The extraction of VC bound lipids after saponification yielded 1.1 ± 0.2% of the total VC weight. Profiles of bound lipids in VC and in SC [16, 19] show similar patterns: fatty acids, ω-hydroxyacids and ω-hydroxyceramides CER(OS) (containing sphingosine) as well as CER(OH) (containing 6-hydroxysphingosine). The ω-hydroxyacids constitutes the major component of lipids bound to the cornified envelope (Fig. 2). Small amounts of ω-hydroxyceramide fraction (probably containing phytosphingosine) with slightly higher R_f value than CER(OH) were detected as well. In contrast to SC, the fatty acid most abundantly present in all analyzed bound lipid fractions is ω-hydroxyeicosanoic acid (Table 3). CER(OS) contains ω-hydroxyacids with chain length up to 34 carbon atoms. These long chain ω-hydroxyacids are only minor components in CER(OH) and the ω-hydroxyacid fraction. Next to α- and ω-hydroxyacids, also small amounts of branched fatty acids were detected in both the CER(OS) and CER(OH) fractions.

Table 3. Composition of bound lipids of vernix caseosa (weight% per fraction, n=3)

A. Overview

compound	CER(OS)	CER(OH)	ω-hydroxy acids
ω -hydroxy acids	75.7	61.6	97.1
α -hydroxy acids	15.1	16.2	2.8
iso	4.4	9.1	-
anteiso	4.9	13.1	

B. Detailed chain length distribution

chain length	CER(OS)	CER(OH)	ω-hydroxy acids
ω-hydroxyacids			
12	-	-	0.7
15	3.4	-	0.6
18	3.7	-	7.8
19	-	-	3.6
20	30.7	28.3	49.3
22	-	14.7	21.1
23	2.2	-	-
24	3.5	18.6	3.1
25	3.7	-	-
26	5.8	-	3.2
28	-	-	5.4
30	8.5	-	0.6
31	4.9	-	-
34	9.3	-	1.7
α-hydroxyacids			
18	-	-	0.4
19	-	-	0.4
20	-	-	2.0
21	2.8	11.0	-
22	1.8	-	-
24	2.9	5.2	-
27	4	-	-
30	1.8	-	-
31	1.8	-	-
iso			-
20	4.4	9.1	-
anteiso			-
22	-	5.0	-
26	4.9	4.1	-
30	-	4.0	-

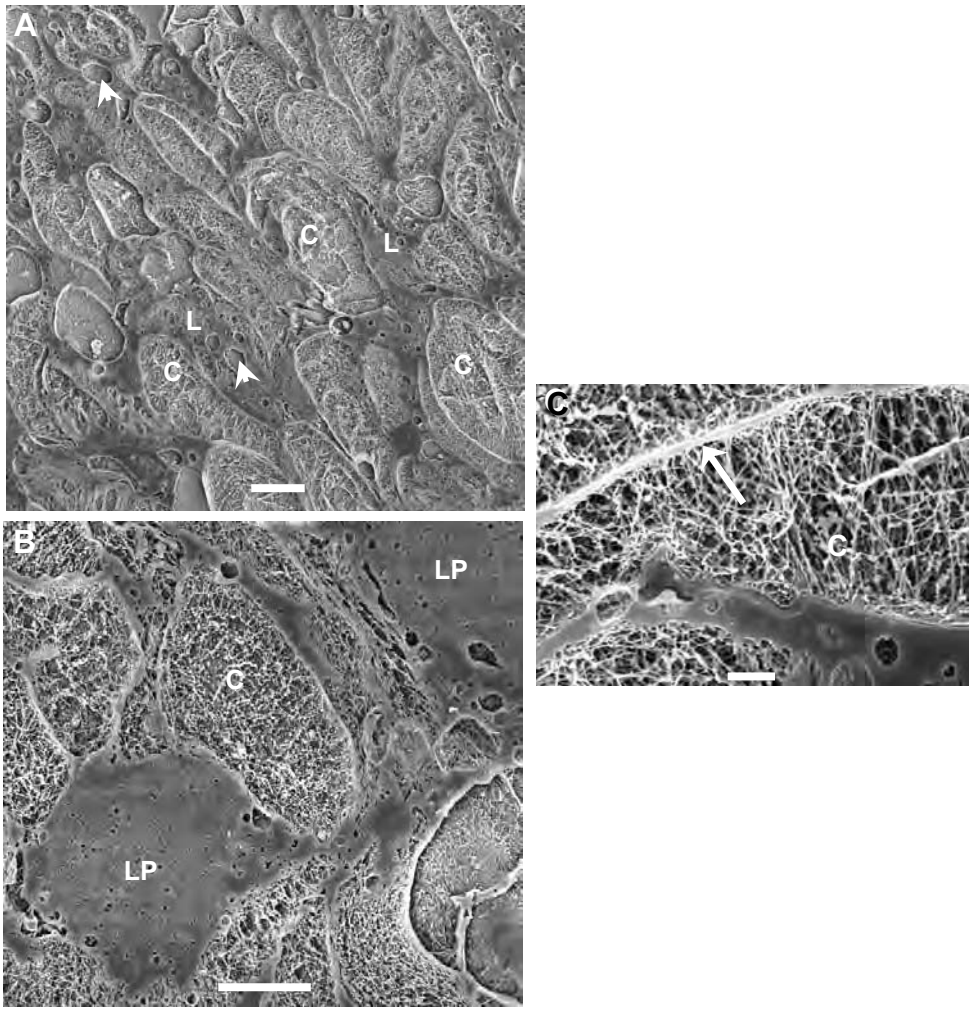

Figure 3. Structure of vernix caseosa is characterized by corneocytes embedded in lipid domains (L). Cryo-SEM pictures of vernix caseosa show corneocytes (panel C), which are surrounded by lipid domains (L). Spherical structures (arrow heads) can also be observed. A certain state of order can be seen (panel A). Lipid material is accumulated between corneocytes and form lipid pools (LP) as depicted in panel B. In panel C the presence of the cornified envelope (arrow) on the boundary of the cell can clearly be distinguished. The inner cellular network consisting of keratin fibres is also clearly visible. *Scale bars* = 10 μm (A), 5 μm (B) and 1 μm (C).

Water is mainly present in the corneocytes, while large intercellular lipid domains are observed in regions of clustered corneocytes

For ultrastructural examinations of the fresh fully hydrated VC, cryo-SEM in combination with cryo-planing has been used. This technique provides the first plane cross-sections of VC as illustrated in figure 3. In general, VC is composed of elliptically shaped corneocytes embedded in a lipid matrix. The longest axis of the cross sections of corneocytes ranges from approximately 15 µm up to 50 µm. figure 3A illustrates the preference of a certain degree of orientation of the corneocytes but the high state of ordering as observed in SC is absent. As depicted in figure 3B and 3C, the interior of the corneocytes is characterized by a network of white fibres, which represents the keratin filament of the cells. In between the keratin, dark regions are observed. These dark regions represent the water domains. In most cases the corneocytes are located closely to each other. However, figure 3A also shows areas with a very smooth appearance located between the cells. These domains correspond to the intercellular lipid regions (L) and are frequently surrounded by several corneocytes. In figure 3B a higher magnification of the lipid domains is shown and the accumulation of lipids to a lipid pool can be observed (LP). Very interestingly, in the lipid domains small round structures are observed (Fig. 3B). As these round structures are very dark in appearance, it most probably represents small water pools within the lipid domains. The cross-section of these structures ranges from 50 nm up to several µm. A higher magnification is shown in figure 3C. In this image the cornified envelope is recognized by a bright, white line surrounding the cell (arrow). Besides the corneocytes also a domain of lipids is observed with the round structures. The dark appearances of these circular structures contain small white dots and fibres. Although the origin is not fully understood, it might represent salt or proteins.

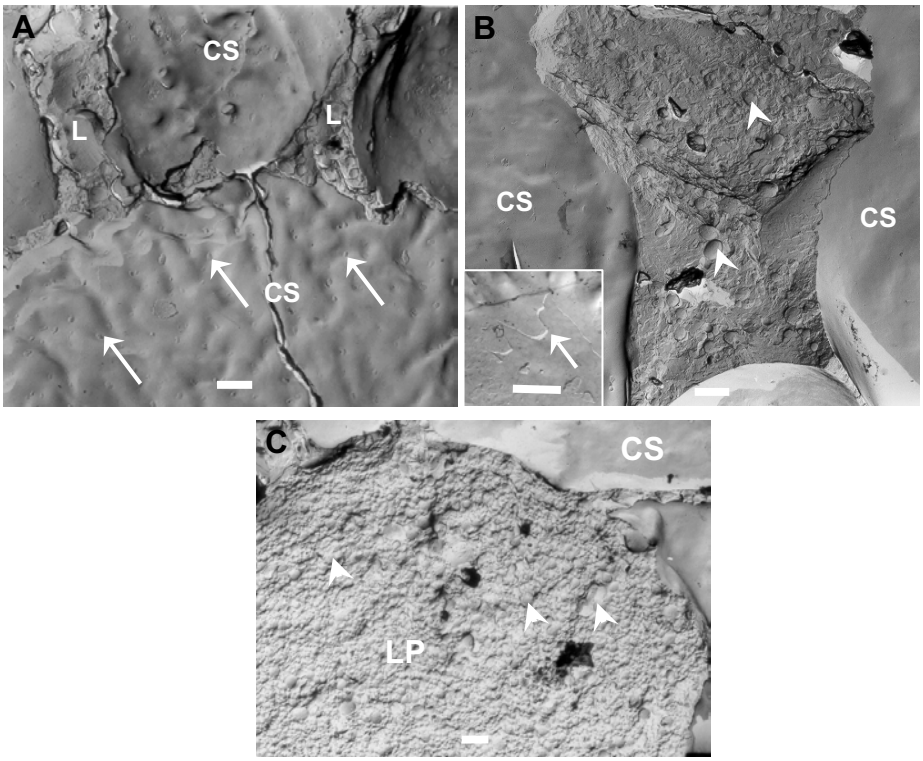

Figure 4. Lipids of vernix caseosa are sandwiched between corneocytes. Photomicrographs obtained by FFEM depict smooth cell surfaces, indicated by CS. Intercellular lipid material has a very heterogeneous appearance (L). In addition, spherical structures could again be observed (arrow heads). Panel A depicts the cell surfaces (CS), characterized by a patchy pattern (arrows), and intercellular lipids (L). The step in the insert in panel B (small arrow) indicates a fracture across a lamellar structure, which only occasionally appeared. A high accumulation of lipids forming a lipid pool (LP) and spherical structures (arrowheads) could be observed in panel C. *Scale bars* = 1µm

Lipids in between VC corneocytes show a heterogeneous appearance and form only occasionally lipid lamellae

A more detailed analysis of the lipid domains can be conducted with FFEM. The images depict mainly surfaces of corneocytes that are characterized by very smooth fracture planes (Fig. 4). This is a consequence of the fracture technique, which always takes the route of least resistance. In figure 4A a cluster of 5 corneocytes, separated by sharp boundaries, is shown. In addition several intercellular lipid domains are visualized. The smooth surfaces of the corneocytes most probably represent the bound lipids. These smooth surfaces very often show a patchy pattern (see arrows in Fig. 4A).

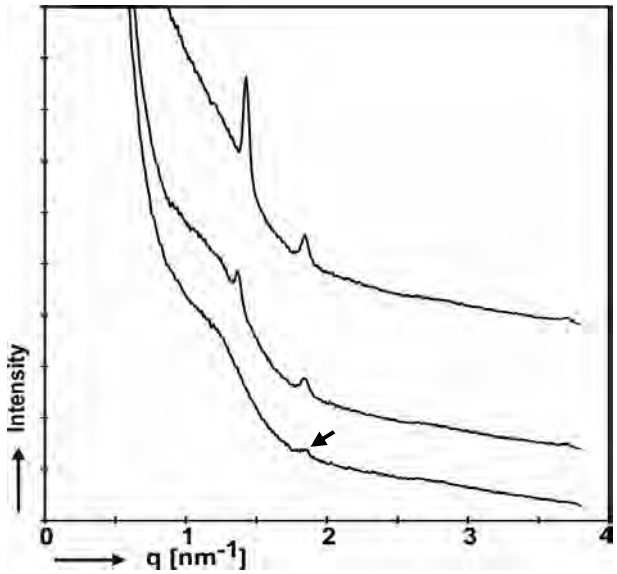

Figure 5. VC shows arbitrary ordering in lipid organization. The small angle X-ray diffraction patterns of three different VC donors clearly show differences in the lipid organization. An ordering indicated by the peaks at q=1.43 nm^{-1} (upper pattern) and at q=1.36 nm^{-1} (middle pattern) could be observed. In addition, those curves show a clear crystalline peak at q=1.85 nm^{-1} caused by cholesterol. Besides a rudimental cholesterol peak (arrow) no ordering could be observed in the third sample (lower pattern).

The lipid regions are characterized by a rough appearance, indicating the absence of a long range ordering of the lipids (Fig. 4B). Only occasionally sharp steps could be observed suggesting the presence of lipid lamellae (insert in Fig. 4B). In the large lipid domains (Fig. 4C), very frequently spherical structures (arrowheads) are observed. No ordered distribution of the spherical structures in space was noticed, suggesting the absence of long range ordering.

No long range ordering of the lipids in VC

The diffraction profiles of the VC obtained from different donors differ slightly (Fig. 5). One out of the three diffraction profiles does not reveal any sharp peaks, while two diffraction profiles exhibit one sharp peak at approximately q=1.43 nm^{-1}and q=1.36 nm^{-1}, respectively. However, as no higher order reflections were observed indicating that no well-defined long range ordering, such as the occurrence of lamellae stacks, is present in these samples. In the three diffraction curves a diffraction peak at q=1.85 nm^{-1} could be identified, which is attributed to crystalline CHOL.

Discussion

It has been suggested that VC protects the fetus of unwanted influences from its environment and might be an important player in promoting the maturation of the SC *in utero*. As the lipid composition and ultrastructure of VC might be crucial for its biological function, information on these properties is of great interest. Although several groups examined the lipid composition of VC, no information is available on the integral lipid composition of VC. Furthermore in several studies fatty acid chains up to a chain length of only 20 C-atoms have been reported to be present in substantial amounts, while it is expected that longer fatty acid chains are also present in VC. In addition, no information is available on the composition of the bound lipids and only limited information is available on the ultrastructure of VC. All these aspects have been addressed in this study and will be discussed below.

Free lipid composition in VC

The present study reveals that only 10% of the VC lipids consists of the barrier lipids (CHOL, FFA and CER), which are the major lipid classes in SC. The remaining 90% of the lipids consist of nonpolar lipids such as SE, WE, TG. Interestingly, the nonpolar part of VC shows similarity with sebaceous lipid profiles, e.g. presence of SQ and high amounts of TG, indicating that VC lipids originate from both, sebaceous glands and keratinocytes [5, 25]. It is known that the sebaceous lipids are secreted in a surge within the last weeks of gestation [26]. Interestingly, it was confirmed that VC of male babies had significant more SE/WE than females (data not shown) [27].

CER composition in VC

Even though the levels of the CER present in SC and VC are very different, the profiles are very similar. All the CER classes that are identified in SC are also observed in VC and the CER composition is comparable with the exception of CER(NP), which shows a much higher level in SC than in VC. Recently, it was described that CER(AH) is the most prevailing CER of VC, followed by CER(AS) and CER(NS) [5], while in our studies the CER most abundantly present are CER(AH), CER(NS) and CER(AS). This difference might be explained by differences in the quantification approach used. While previously CER(NP) and CER(AS) were used as standard to determine the levels of all individual CER [5], in the present study five synthetic CER subclasses resembling the natural CER very closely were used as standards for quantification purposes. Furthermore, our lipid analysis revealed significant lower relative amount of barrier lipids than reported in the previous study.

Fatty acid profile in VC

The distribution of the fatty acids observed in the present study is similar to that reported earlier [7-11]. However, our results clearly demonstrate that fatty acids with chain lengths beyond 20 C-atoms comprise an important fatty acid population in VC. These long chain fatty acids were often neglected in the earlier studies. Besides iso- and anteiso fatty acids, cis- and trans- isomers of monounsaturated fatty acids could be identified. The presence of unsaturated fatty acids increases the diversity because not only different positions of the double bond [11, 28] are observed, but also different stereo-isomer analogs are present. Our results also illustrate that fatty acids with shorter chain length (C16-C18) are prevailing in TG and WE fractions, while very long chain fatty acids (>C20) are the major fatty acids of the SE fraction. Moreover, we observed that the branched/straight ratio of fatty acids is decreasing with lipid polarity, being the highest in the least polar SE and decreasing in more polar components, such as TG and FFA. Only the fraction of DIOL does not fully follow this trend. When comparing our results with those of Tollin *et al.* [13], it can be noticed that in our VC samples the main FFA fractions are C16:0, C16:1t, C15:0 and C18:1t, while the most abundant ones in their VC samples are C16:0, C24:0, C18:2 and C18:1. Furthermore, we did not observe polyunsaturated fractions of FFA, while they did not notice branched fatty acids.

Bound lipids

As VC consists of the hydrated hydrophilic corneocytes surrounded by lipophilic intercellular lipids, the interface of both domains has an important mediating function. In SC this interface is formed by lipids covalently bound to the cornified envelope (corneocyte-bound lipid envelope [29]). Our results demonstrate for the first time that in VC - like in SC - bound lipids are present that are covalently linked to the cornified envelope. The bound lipids mainly consist of four lipid classes, namely ω-hydroxyacids, fatty acids and the ω-hydoxy-CER, CER(OS) and CER(OH), similarly as observed in SC [29]. However, the chain lengths of the bound lipids in VC are different from those in SC. Striking is the high level of ω-hydroxyeicosanoic acid (Table 3B) in these lipids, while the ω-hydroxyacids with 30 C-atoms, abundantly present in SC [16], is almost absent in VC. Noticeable is also the presence of branched subtypes of fatty acids in CER(OS) and CER(OH). Oku *et al.* [12] described also the presence of branched fatty acids in the CER of free VC lipids.

Ultrastructure of VC

Cryo-SEM in combination with slicing and planing provides very flat surfaces across hydrophilic as well as lipophilic domains and thus provides structural

information about both domains. FFEM reveals fracture planes of the VC samples, in which the fracture planes run through the regions of least resistance, which are mainly the lipid domains. Additionally to the study of Pickens *et al.* [4], the cryo-SEM images depict the internal structure of the corneocytes and reveal that the keratin filaments constitute the scaffold and create a body to store water within the corneocytes. Furthermore, the corneocytes show a certain degree of orientation in the VC samples. In the extracellular regions lipids are present similarly as in SC. The lipid domains are characterized by smooth regions in the cryo-SEM images with many small round structures (Fig. 3B and 3C). These structures were also described in the earlier study [4]. The origin and function of the round structures remain unclear. A former study showed the presence of antimicrobial peptides in such inclusion bodies [30] but their larger size might be explained by coalescence induced by their technique. However, we propose that the inner content most probably consist of water, which is identified by cryo-SEM as small dark holes. This might explain the round shaped structure, as a high surface tension, normally observed between the lipophilic domains and the hydrophilic water, will minimize the interfacial surface creating these round shaped structures. At higher magnification (Fig. 3C) it is clearly observed that besides water, other material is present in these little water pools. This might be proteins, peptides or salt crystals of which the biological functions still remain unclear.

Cryo-SEM and FFEM reveal the presence of large lipid pools (Fig. 3B and 4B) in regions of clustered corneocytes. Such large regions of lipids have not been observed in SC and might partially be due to the absence of corneodesmosomes in VC allowing separation of the corneocytes. In the lipid regions many small spherical particles are observed with FFEM (Fig. 4B and 4C). Most probably these represent the round shaped structures identified with cryo-SEM, but now fractured along the outer surface of the particles, which seems to be of lipid nature. In addition the lipid domains show a very heterogeneous and rough appearance (Fig. 4B) indicating that lipids are not highly organized. Only on the cell surfaces (insert Fig. 4B), lipid lamellae could be observed occasionally. This is different from the lipids in SC, which are organized in very well defined stacks of lipid lamellae [31]. The results of the SAXD studies corroborate these results. At the diffraction profiles, only 2 out of the 3 diffraction patterns reveal one additional diffraction peak, next to the peak attributed to crystalline CHOL, indicating the absence of long range ordering.

The difference in organization in VC and SC can be explained by the difference in lipid composition at least in two ways. I) Barrier lipids, especially CER with long fatty acid chains play an important role in the characteristic organization in

SC [32]. Most probably, the lower level of this lipid class in VC reduces its contribution to the final lipid organization. II) In SC the majority of the lipids have straight unsaturated fatty acid chains, while in VC the majority of the fatty acid chains are either unsaturated or branched. This most probably will have important consequences for the lipid organization. However, in order to draw any final conclusions about the specific role of the reduced CER level and the increased levels of branched and unsaturated fatty acids more studies are required to address this issue. Those could also include gestational-period dependent changes in VC lipid composition as developmental differences in VC may play an important role for the properties.

What have we learned from these studies about the formation, origin and function of VC? As far as the lipid composition is concerned, only a low content of barrier lipids is present in VC. This might suggest that the primary function of VC is not only to limit the diffusion of substances across VC, but also to protect the initially formed SC of the fetus from direct contact with the amniotic fluid. This might also facilitate the formation of a mature SC *in utero*. The synthesis of barrier lipids and chemical linkage of the bound lipids to the cornified envelope is a very characteristic process for terminal differentiation in the epidermis. One can speculate that the SC present in the infundibular region of the sebaceous glands is the source of the VC corneocytes and of the barrier lipids. In this region corneocytes and intercellular lipids mix with the sebaceous lipids within the pilosebaceous units and spread out around the opening of the hair follicle. In fact this process is confirmed by the observation with FFEM, which revealed that the disordered lipid structures (supposedly nonpolar sebaceous lipids) are mainly located in the intercellular lipid pools, while the ordered structures (supposedly barrier lipids) such as lamellae are located close to the surface of the corneocytes. The VC corneocytes, lacking desmosomes and having shorter-chain bound lipids, slightly differ from the SC corneocytes. Interestingly, the absence of desmosomes might facilitate the desquamation process enriching the VC with corneocytes. As demonstrated by the cryo-SEM images, corneocytes have an important function in retaining water in VC. The delivery of water from VC to the underlying epidermis might affect the terminal differentiation process. In this respect the water transport from the corneocytes to the surrounding lipid regions may be regulated by bound lipids.

In summary, although some similarities have been observed between the structures of SC and VC, major differences are also observed. The composition and organization of the free lipids in VC for example support a probable origin

in the pilosebaceous glands. VC corneocytes are not linked together via corneodesmosomes and the intercorneocyte lipids are not structured into lamellae although a diffuse pattern of possible 'water droplets' was noted, distributed within the lipid matrix. The composition of the lipids bound to the cornified envelope is very similar between SC and VC, except for the length of fatty acid chains. The functional significance of these structural and compositional differences and the multiple possible roles of VC during the last trimester of gestation and during transition to the postnatal environment remain to be further explored.

References

[1] Hardman MJ, Moore L, Ferguson MW, Byrne C. Barrier formation in the human fetus is patterned. *J Invest Dermatol* 1999 Dec;113(6):1106-13.

[2] Haubrich KA. Role of Vernix caseosa in the neonate: potential application in the adult population. *AACN Clin Issues* 2003 Nov;14(4):457-64.

[3] Agorastos T, Hollweg G, Grussendorf EI, Papaloucas A. Features of vernix caseosa cells. *Am J Perinatol* 1988 Jul;5(3):253-9.

[4] Pickens WL, Warner RR, Boissy YL, Boissy RE, Hoath SB. Characterization of vernix caseosa: water content, morphology, and elemental analysis. *J Invest Dermatol* 2000 Nov;115(5):875-81.

[5] Hoeger PH, Schreiner V, Klaassen IA, Enzmann CC, Friedrichs K, Bleck O. Epidermal barrier lipids in human vernix caseosa: corresponding ceramide pattern in vernix and fetal skin. *Br J Dermatol* 2002 Feb;146(2):194-201.

[6] Bouwstra JA, Gooris GS, van der Spek JA, Bras W. Structural investigations of human stratum corneum by small-angle X-ray scattering. *J Invest Dermatol* 1991 Dec;97(6):1005-12.

[7] Haahti E, Nikkari T, Salmi AM, Laaksonen AL. Fatty acids of vernix caseosa. *Scand J Clin Lab Invest* 1961;13:70-3.

[8] Kaerkkaeinen J, Nikkari T, Ruponen S, Haahti E. Lipids Of Vernix Caseosa. *J Invest Dermatol* 1965 May;44:333-8.

[9] Fu HC, Nicolaides N. The structure of alkane diols of diesters in vernix caseosa lipids. *Lipids* 1969 Mar;4(2):170-5.

[10] Nicolaides N, Fu HC, Ansari MN, Rice GR. The fatty acids of wax esters and sterol esters from vernix caseosa and from human skin surface lipid. *Lipids* 1972 Aug;7(8):506-17.

[11] Nicolaides N, Ray T. Skin Lipids. 3. Fatty Chains In Skin Lipids. The Use Of Vernix Caseosa To Differentiate Between Endogenous And Exogenous Components In Human Skin Surface Lipid. *J Am Oil Chem Soc* 1965 Aug;42:702-7.

[12] Oku H, Mimura K, Tokitsu Y, Onaga K, Iwasaki H, Chinen I. Biased distribution of the branched-chain fatty acids in ceramides of vernix caseosa. *Lipids* 2000 Apr;35(4):373-81.

[13] Tollin M, Bergsson G, Kai-Larsen Y, Lengqvist J, Sjovall J, Griffiths W, Skuladottir GV, Haraldsson A, et al. Vernix caseosa as a multi-component defence system based on polypeptides, lipids and their interactions. *Cell Mol Life Sci* 2005 Oct;62(19-20):2390-9.

[14] Nugroho AK, Li GL, Danhof M, Bouwstra JA. Transdermal iontophoresis of rotigotine across human stratum corneum in vitro: influence of pH and NaCl concentration. *Pharm Res* 2004 May;21(5):844-50.

[15] Bligh EG, Dyer WJ. A rapid method of total lipid extraction and purification. *Can J Biochem Physiol* 1959 Aug;37(8):911-7.

[16] Wertz PW, Madison KC, Downing DT. Covalently bound lipids of human stratum corneum. *J Invest Dermatol* 1989 Jan;92(1):109-11.

[17] Ponec M, Weerheim A, Lankhorst P, Wertz P. New acylceramide in native and reconstructed epidermis. *J Invest Dermatol* 2003 Apr;120(4):581-8.

[18] Motta S, Monti M, Sesana S, Caputo R, Carelli S, Ghidoni R. Ceramide composition of psoriatic scale. *Biochim Biophysic Acta* 1993;1182:147-51.

[19] Ponec M, Boelsma E, Weerheim A. Covalently bound lipids in reconstructed human epithelia. *Acta Derm Venereol* 2000 Mar-Apr;80(2):89-93.

[20] Ponec M, Weerheim A, Kempenaar J, Elias PM, Williams ML. Differentiation of cultured human keratinocytes: effect of culture conditions on lipid composition of normal vs. malignant cells. *In Vitro Cell Dev Biol* 1989 Aug;25(8):689-96.

[21] Bouwstra JA, de Graaff A, Gooris GS, Nijsse J, Wiechers JW, van Aelst AC. Water distribution and related morphology in human stratum corneum at different hydration levels. *J Invest Dermatol* 2003 May;120(5):750-8.

[22] Honeywell-Nguyen PL, de Graaff AM, Groenink HW, Bouwstra JA. The in vivo and in vitro interactions of elastic and rigid vesicles with human skin. *Biochim Biophys Acta* 2002 Nov 14;1573(2):130-40.

[23] Bras W. 1998. A SAXS/WAXS beamline at the ESRF and future experiments. *J Macromol Sci Phys B* 1998;37:557-66.

[24] de Jager M, Gooris G, Ponec M, Bouwstra J. Acylceramide head group architecture affects lipid organization in synthetic ceramide mixtures. *J Invest Dermatol* 2004 Nov;123(5):911-6.

[25] Stewart ME, Quinn MA, Downing DT. Variability in the fatty acid composition of wax esters from vernix caseosa and its possible relation to sebaceous gland activity. *J Invest Dermatol* 1982 Apr;78(4):291-5.

[26] Wysocki SJ, Grauaug A, O'Neill G, Hahnel R. Lipids in forehead vernix from newborn infants. *Biol Neonate* 1981;39(5-6):300-4.

[27] Nazzaro-Porro M, Passi S, Boniforti L, Belsito F. Effects of aging on fatty acids in skin surface lipids. *J Invest Dermatol* 1979 Jul;73(1):112-7.

[28] Downing DT, Greene RS. Double bond positions in the unsaturated fatty acids of vernix caseosa. *J Invest Dermatol* 1968 May;50(5):380-6.

[29] Swartzendruber DC, Wertz PW, Madison KC, Downing DT. Evidence that the corneocyte has a chemically bound lipid envelope. *J Invest Dermatol* 1987 Jun;88(6):709-13.

[30] Akinbi HT, Narendran V, Pass AK, Markart P, Hoath SB. Host defense proteins in vernix caseosa and amniotic fluid. *Am J Obstet Gynecol* 2004 Dec;191(6):2090-6.

[31] Madison KC, Swartzendruber DC, Wertz PW, Downing DT. Presence of intact intercellular lipid lamellae in the upper layers of the stratum corneum. *J Invest Dermatol* 1987 Jun;88(6):714-8.

[32] Bouwstra JA, Gooris GS, Dubbelaar FE, Weerheim AM, Ijzerman AP, Ponec M. Role of ceramide 1 in the molecular organization of the stratum corneum lipids. *J Lipid Res* 1998 Jan;39(1):186-96.